Journal of Applied Automation Technologies

Research Paper

Autonomous Driving Path Planning Under Adverse Weather Based on Generative Adversarial Networks

Sabina Walczak[1], Patrycja Ostrowska[1,*] and Lidia Wójcikowa[1]

[1] Faculty of Electrical Engineering, Automatics, Computer Science and Biomedical Engineering, AGH University of Science and Technology, Krakow, 30-059, Poland
*Corresponding author: patrycja.os@agh.edu.pl

Abstract. Due to decreased lane perception, obstacle localization, and decreased confidence in the drivable area brought on by rain, fog, snow, and poor light, autonomous driving path planning is significantly hampered in inclement weather. This research proposes a generative adversarial network-based path planning paradigm for autonomous driving in inclement weather to improve planning resilience. First, weather-degraded driving scenarios that preserve the obstacle structure and road geometry are created via conditional adversarial generation. A weather-aware risk representation is then created based on the lane-boundary confidence, obstacle likelihood, visibility attenuation, and road-surface adhesion risk. Lastly, feasible pathways under perceptual uncertainty are produced by a stable trajectory optimization technique. The suggested approach decreased the mean path deviation from 0.47m to 0.31m, raised the obstacle avoidance success rate from 84.6% to 94.1%, and decreased the planning failure rate by 18.6% in dense fog and heavy rain, according to tests conducted in a simulated and actual adverse weather driving environment. The tests demonstrate how adversarial weather generation might enhance driving safety by extending planning to invisible settings.

Keywords: *Generative Adversarial Network, Autonomous Driving, Path Planning, Adverse Weather, Robust Planning*

Received on 24 April 2023, Accepted on 29 September 2023, Published on 15 October 2023

Introduction

The autonomous driving route planning module generates realistic driving trajectories using the outputs of perception and localization, then confirms that these trajectories can safely navigate a complex traffic scenario. Lane boundaries, road signs, curb structures, cars, pedestrians, and free-space areas can all be recognized with a fair amount of certainty in excellent weather. Rain streaks, fog dispersion, snow occlusion, water reflection, poor light, etc. can all reduce contrast and change the spatial elements that the designer needs in inclement weather. Research on self-driving cars reveals that these vehicles' sensing capabilities and operating uncertainty drastically decline in inclement weather, such as rain, snow, fog, and hail [1]. The precision and stability of the upstream perception in open and dynamic driving situations have a direct impact on planning dependability, according to additional study on autonomous driving systems [2].

Graph search, sampling-based planning, model predictive control, and optimization-based trajectory generation are examples of classic path-planning techniques that often make the assumption that the obstacle state and road geometry are precisely known. In inclement weather, the presumptions are rather weak. Drivable-area segmentation may be inconsistent, obstacle boxes may be overlooked or delayed, and lane detection may be erratic. Motion planners can still generate a somewhat smooth path, but it may deviate from the poorly perceived lane limit or approach ambiguous barriers too closely. Planners must be exposed to degraded sceneries rather of being trained just in clear-weather scenarios in order to improve robustness, according to recent research on adverse-weather driving, perceptual enhancement, and weather-aware data augmentation

https://doi.org/10.64972/jaat.2023v1.308p22e:294-306

[3]. A useful method for extending uncommon weather situations and minimizing domain shift between typical training data and weather-degraded deployment scenes is to use generative models [4].

Path Planning using Generative Adversarial Networks for Autonomous Driving in Inclement Weather. In order to create rain, fog, snow, and low-light driving circumstances while maintaining the original road layout and obstacle relations, the system will use conditional adversarial generation. Lane confidence, obstruction likelihood, visibility decay, and road-surface adhesion risk are all quantified using weather-aware risk representation. A stable Trajectory Optimization module will produce a route that satisfies a vehicle's kinematic restrictions while avoiding a high-risk area. Reduce the impact of weather bias and enhance planning stability and safety in the case of noisy or insufficient perception data.

Related Work

Autonomous Driving Path Planning Under Uncertainty

Search-based, sampling-based, optimization-based, and learning-based methods have all been researched for autonomous driving path planning. While sampling-based techniques like RRT* are better suited for high-dimensional environments, traditional graph search algorithms like A* and hybrid A* are used to identify deterministic paths in organized road networks. A motion planning survey states that planners must concurrently handle lane limits, moving barriers, interaction uncertainty, and real-time feasibility for highway and urban autonomous driving [5]. Dynamic Obstacle and Lane Mapping Additionally, avoidance methods demonstrate that timely modifications to the drivable-space border have a significant impact on planning performance [6]. As a result, risk-aware path planning has emerged as a significant area of study. The planner must avoid environmental barriers as well as unpredictable elements like human behavior, obscured areas, and even a loss of perceptual confidence [7]. An extension of the concept is game-theoretic planning, which predicts how interactive choices will impact the future course and models other drivers' risk preferences [8].

Adverse Weather Perception and Driving Scene Understanding

A different kind of planning uncertainty is caused by adverse weather, since the planner must consider impaired perception evidence before choosing a trajectory. Long-range depth estimation can be weakened, obstacle shapes distorted, and lane-boundary visibility reduced by rain streaks, fog scattering, snow cover, wet-road reflection, and poor light. Perception systems trained primarily on clear-weather samples perform poorly in poor-weather conditions, according to multi-weather driving datasets [9]. Prior to implementing weather-specific perception or planning techniques, the environment must be recognized, according to studies on weather and light-level classification [10]. Although the goal of perception-friendly enhancement techniques is to restore important visual information in recordings of inclement weather, the planner may still need to resolve some uncertainty in these augmented images [11]. In autonomous driving under different conditions, recurrent conditional generative adversarial networks have been used to model sensor sequences and produce driving-related observations [12]. Conditional image translation techniques are particularly helpful for weather robustness training because they can translate driving scenarios from clear weather to bad weather while maintaining the semantic road structure [13]. Without requiring repetitive manual annotation, multi-domain conditional image translation increases the diversity of training data by producing different adverse-weather styles from a single source scene [14]. The issue that the generated weather images may seem realistic but fail to preserve all safety-critical structures, like as lane markers and object boundaries, has also been addressed by uncertainty-aware GANs [15]. Additionally, rather than merely accomplishing visual style transfer, GAN-based ensemble weather prediction suggests that adversarial generation might represent unpredictable environmental distributions [16].

GAN-Based Scene Generation and Robust Planning Optimization

The usefulness of Generative Adversarial Networks for autonomous driving depends on whether the generated samples can enable safer downstream planning. However, they can be used to generate uncommon and challenging driving scenarios that are not well-represented in real-world datasets. By introducing learned scene priors, sampling-based path planning with generative adversarial heuristics has been used to direct the search in complex constrained environments toward a practical and secure solution [17]. Compared to typical route

https://doi.org/10.64972/jaat.2023v1.308p22e:294-306

optimization, safe motion planning based on adversarial road models can also increase planners' resilience in challenging road circumstances [18]. Instead of relying solely on geometric maps, perception-aware path planning employs neural feature fusion in the planning stage to respond more sensitively to changes in the local environment by taking uncertain environmental evidence into account [19]. Dynamic driving restrictions have been incorporated to the planning aim by research on model predictive trajectory planning, but their practical use necessitates accurate assessment of the road and obstacle condition [20]. When topography or boundary information is not available, robust path execution must simultaneously execute trajectory generating and tracking control, as demonstrated by adaptive trajectory planning for autonomous wheel loaders [21]. Planning frameworks for both structured and unstructured roads also demonstrate that scene representation must adapt to the road's regularity, obstacle density, and map completeness [22]. Constraint relaxation can lessen infeasibility, according to minimum-violation planning and model predictive control comparisons, but the safety margin will be diminished if weather-related uncertainty cannot be disregarded [23]. Road geometry and traffic participant behavior should be taken into account while selecting a safe route, according to behavior assessment of structural urban roads [24]. Cooperative trajectory planning based on nonlinear model predictive control is another technique to improve the path's viability in an interactive traffic environment [25]. Planning delay and vehicle response stability are issues in low-adhesion road conditions, as demonstrated by real-time predictive control for simultaneous drift and trajectory tracking [26]. The created scenarios must also adhere to practical traffic interaction regulations, according to research on autonomous intersection trajectory planning; otherwise, the synthetic variability will result in irrational planning labeling [27]. Weather deterioration should be modeled with sensor-specific uncertainty rather than being treated as a straightforward image-noise problem, as demonstrated by polarized camera recognition in inclement weather [28]. Research on automotive radar perception in inclement weather has also demonstrated that other sensor modules can be employed to augment the camera when its confidence is low [29]. Geometric reasoning and path planning will be harmed by weather-induced visual noise that affects depth perception from a noisy camera sensor [30].

GAN-Enhanced Robust Path Planning Method

Adverse Weather Scene Generation Framework

In order to replicate the rain, fog, snow, and low light circumstances of driving scenes in clear weather, the suggested method first builds a weather generating network. Give the original image, semantic road mask, obstacle layout, and weather code to the generator. Check to see if the created scene is visually aligned with the specified weather domain and if the road geometry has an appropriate structure. The GAN-based system for creating bad weather scenes is shown in Figure 1. Because path planning must maintain the road layout and obstacle locations, the design does not employ unrestricted style transfer.

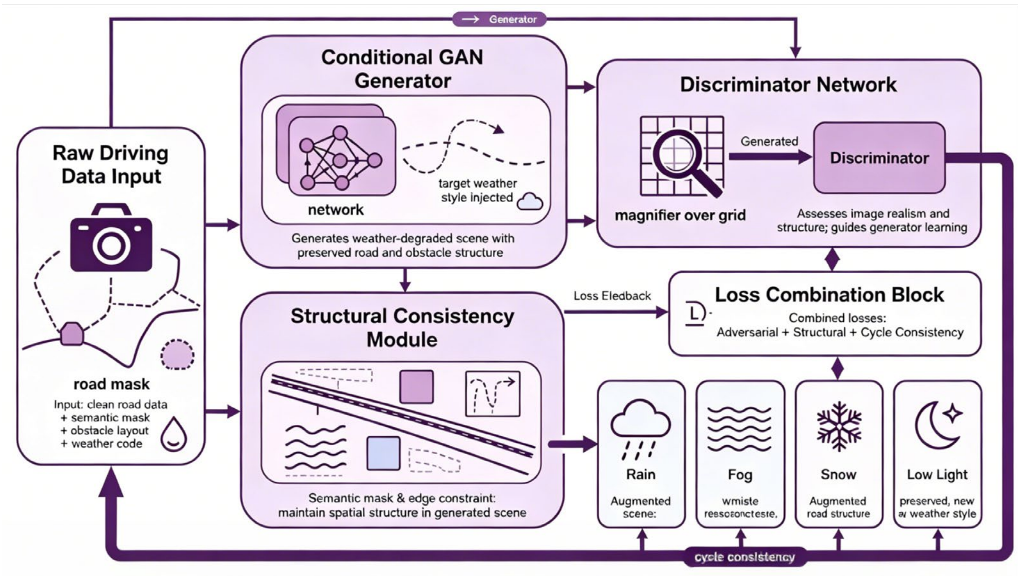

Figure 1. GAN-based adverse weather scene generation framework

The adversarial generation objective is designed to make the generated image close to the target weather distribution while keeping the source road structure stable.

$$L_{\mathrm{adv}} = \mathbb{E}[\log D(y,w)] + \mathbb{E}[\log(1 - D(G(x,w),w))] \quad \text{Eq.(1)}$$

Only adversarial realism is insufficient for planning. A rainy or foggy image may look realistic but distort lane boundaries or obstacle locations. Therefore, a structural preservation term constrains the generated scene using semantic masks and edge responses extracted from the source image.

$$L_{\mathrm{str}} = \|M(G(x,w)) - M(x)\|_1 + \beta\|E(G(x,w)) - E(x)\|_1 \quad \text{Eq.(2)}$$

The final weather generation loss combines adversarial realism, structural preservation, and cycle consistency. This makes the generated scenes useful for planner training because visual degradation is added without destroying the spatial relations needed for trajectory reasoning.

$$L_G = L_{\mathrm{adv}} + \lambda_s L_{\mathrm{str}} + \lambda_c\|G(G(x,w),w_0) - x\|_1 \quad \text{Eq.(3)}$$

In the implementation, four weather domains are used: rain, fog, snow, and low illumination. Each clear scene is translated into three to four degraded variants. The generated samples increase the training set from 18,400 clearweather frames to 73,600 weather-diverse frames.

Weather-Aware Risk Representation

The second module converts weather-degraded perception into a compact risk representation for planning. Instead of directly using generated images as planner input, the method estimates lane-boundary confidence, obstacle occupancy probability, visibility attenuation, and road-surface adhesion risk.

$$C_{\mathrm{lane}}(p) = \sigma(a_1 B(p) + a_2 S(p) - a_3 V_w) \quad \text{Eq.(4)}$$

Here, boundary evidence, semantic road support, and weather-induced visibility loss jointly determine whether a grid cell should be treated as reliable lane space.

$$P_{\mathrm{obs}}(p) = 1 - \prod_k \left(1 - q_k \exp(-\|p - o_k\|^2 / r_k)\right) \quad \text{Eq.(5)}$$

The obstacle probability combines all detected objects and expands uncertainty when object localization becomes less reliable under fog, rain, or snow.

$$R_{\mathrm{vis}}(p) = \exp(-d_w(p)/\kappa_w) \quad \text{Eq.(6)}$$

The visibility term describes how far reliable perception can extend under the current weather condition. Dense fog and heavy rain produce a faster decay.

$$R_w(p) = \alpha(1 - C_{\mathrm{lane}}(p)) + \eta P_{\mathrm{obs}}(p) + \gamma(1 - R_{\mathrm{vis}}(p)) + \delta A_{\mathrm{road}}(p) \quad \text{Eq.(7)}$$

Figure 2 presents how the risk representation is connected with robust trajectory optimization.

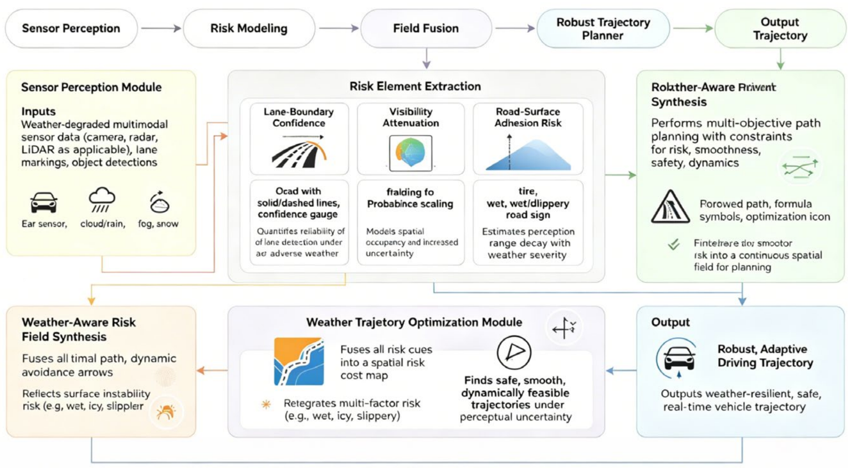

Figure 2. Weather-aware risk representation and robust trajectory optimization module

Robust Trajectory Optimization Strategy

The planning module searches for a trajectory that is safe, smooth, and dynamically feasible under weather uncertainty. A candidate trajectory is represented by a sequence of states containing position, heading, velocity, and steering angle.

$$J_{\text{risk}}(\tau) = \sum_{t} R_w(p_t)\exp(-d_t/\rho) \quad \text{Eq.(8)}$$

The risk cost accumulates weather-aware risk along the candidate path, preventing the planner from ignoring high-risk cells near the vehicle.

$$J_{\text{smooth}}(\tau) = \sum_{t} \|p_{t+1} - 2p_t + p_{t-1}\|^2 \quad \text{Eq.(9)}$$

The smoothness cost penalizes abrupt curvature change, which is important under slippery road conditions because aggressive steering may lead to tracking instability.

$$\tau^* = \arg\min_{\tau}\left(J_{\text{risk}} + \mu J_{\text{smooth}} + \nu J_{\text{safe}} + \xi J_{\text{dyn}}\right) \quad \text{Eq.(10)}$$

The optimal trajectory minimizes the weighted objective under vehicle kinematic constraints. Compared with ordinary clear-weather planning, the proposed objective explicitly shifts the path away from visually ambiguous lanes and uncertain obstacles.

Experimental Scheme and Quantitative Evaluation

Dataset Construction and Implementation Details

The experiment's mixed dataset consists of both created weather-augmented scenarios and actual driving situations in bad weather. Frames from urban roads, suburban roads, intersections, and highways are used when there is no inclement weather. 4,200 rainy, 3,600 foggy, 2,800 snowy, and 2,400 low-light shots make up the actual weather samples. The weather training set is expanded to 73,600 frames using conditional GAN generation. A 60 m by 20 m local grid with a 0.2 m resolution makes up the Planning Region. Optimize the planner using a batch size of 16 trajectory samples after training the generator for 80 epochs.

$$D_{\text{aug}} = \{(x_i, w_i, y_i)\}_i \cup \left\{\left(G(x_i, w_j), w_j, y_i\right)\right\}_{ij} \quad \text{Eq.(11)}$$

The augmented dataset keeps the planning label unchanged because generated weather changes visual appearance rather than road topology. This setting allows the planner to learn how the same path should be selected when perception quality deteriorates.

Evaluation Indicators for Planning Robustness

Planning performance is evaluated from accuracy, safety, smoothness, and real-time efficiency. The first metric is average path deviation, which measures the distance between the generated trajectory and the expert or highconfidence reference trajectory.

$$E_{\text{path}} = \frac{1}{T}\sum_{t} \left\|p_t - p_{\text{ref},t}\right\|^2 \quad \text{Eq.(12)}$$

Safety is evaluated by obstacle avoidance success rate and collision rate. A planning trial is counted as successful when the generated path avoids all annotated obstacles and remains within the drivable area.

$$S_{\text{avoid}} = \frac{N_s}{N_s + N_c + N_f} \quad \text{Eq.(13)}$$

Trajectory smoothness is measured by the accumulated curvature variation. This metric is important because weatherdegraded road surfaces require stable steering and moderate lateral acceleration.

https://doi.org/10.64972/jaat.2023v1.308p22e:294-306

$$C_s = \frac{1}{T}\sum_{t} |\kappa_t - \kappa_{t-1}| \quad \text{Eq.(14)}$$

The mean planning delay reflects real-time feasibility. The objective upper bound of the test platform is 50 ms per planning cycle, and the entire framework of risk representation and trajectory optimization must function inside the autonomous driving stack's decision interval.

Comparative Experimental Design

Five baselines are used to compare the suggested method: Deep reinforcement learning planners, A* with static obstacle cost, RRT* with collision checking, model predictive control without weather risk, and a planner trained without GAN-generated scenes. The local map size and perceptual output are the same for every approach. Evaluations are conducted in low light, fog, snow, rain, and clear weather. Only produced data are utilized for training and validation, and real weather samples are retained for the test set to avoid overfitting to a single synthetic distribution. By contrast, ascertain whether adversarial weather augmentation and weather-aware risk representation improve path stability in situations where perception confidence is diminished.

Result Interpretation and Comparative Analysis

Overall, Path Planning Performance Analysis

Both the lateral planning error and the failure rate are generally larger in bad weather; the perceptual confidence abruptly declines in fog, rain, and low light. A*, RRT*, MPC, DRL planner, and the suggested approach all had average path deviations of 0.34, 0.38, 0.29, 0.32, and 0.27 meters in favorable conditions. These values are, respectively, 0.71 m, 0.68 m, 0.54 m, 0.49 m, and 0.33 m in the dense fog. There is a performance gap, meaning that the traditional planner is less dependable when the source of visual uncertainty shifts and the reliability of lane and obstacle data declines, even though it can still produce a workable geometric path. End-to-end driving models need explicit uncertainty treatment when the training and testing distributions are different, as demonstrated by robust sim-to-real investigations [31]. The overall planning performance in various weather conditions is depicted in Figure 3. Figure 3(a) compares the path deviation for the five planning methods, Figure 3(b) shows the success rate of obstacle avoidance in both clear and adverse weather, and Figure 3(c) shows the failure rate of planning in rain, fog, snow, and low light.

When compared to the best non-GAN baseline, the suggested technique reduces the average deviation caused by adverse weather from 0.47 m to 0.31 m. The suggested method's obstacle avoidance success rate is 94.1%, MPC's is 87.5%, and DRL planner's is 89.3%. The weather-aware risk field shifts the planned trajectory away from regions with unstable obstacle localization confidence since the improvement is most noticeable in dense fog and heavy rain. The notion that generating information should be linked to safety-oriented decision factors rather than being used as additional visual samples is further supported by driving risk prediction research based on GAN-based traffic models [32].

Weather Robustness and Risk Response Analysis

Additional explanations for the more stable trajectories of the suggested planner under reduced perception can be found in weather-specific study. After 35 meters, dense fog lowers the long-range obstacle confidence, making it difficult for conventional planners to predict the collision risk. When it rains a lot, reflective road surfaces increase lateral path fluctuation by causing discontinuous object-box oscillation. Because road borders and markers are partially obscured in snowy circumstances, lane-boundary confidence declines. These weather impacts are systematic alterations in semantic reliability rather than random visual disturbances, according to adverse-condition scene understanding criteria [33]. The algorithm's resilience to rain, fog, and snow disturbances is demonstrated in Figure 4. Figure 4(a) illustrates the stability of dense-fog planning under long-range visibility decay, Figure 4(b) illustrates how heavy rain modifies the obstacle-risk response near reflective road regions, and Figure 4(c) contrasts the dependability of lane boundaries on snow-covered roads.

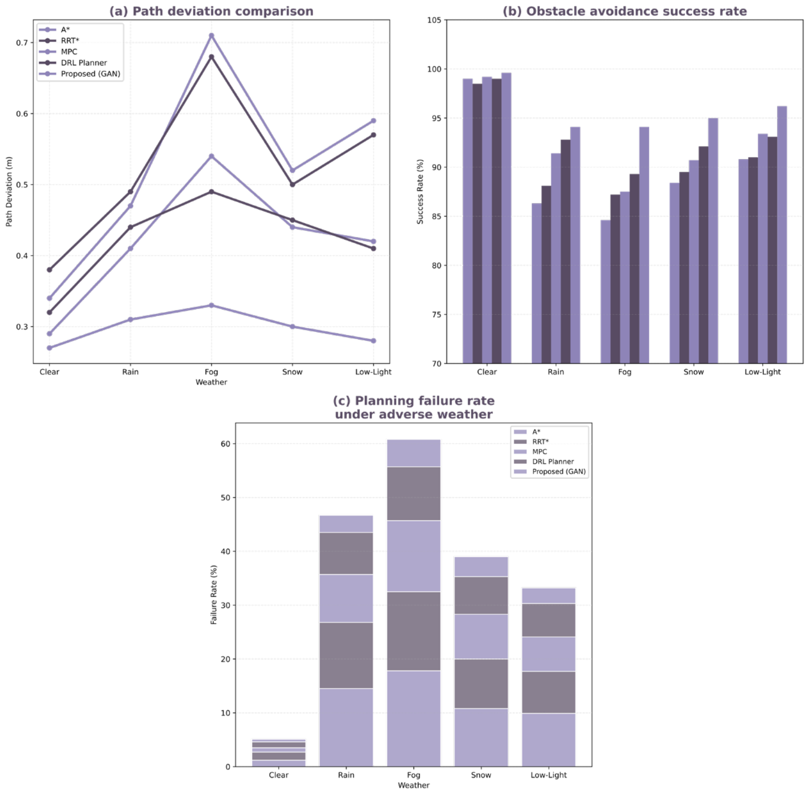

Figure 3. Overall planning performance under different weather conditions. (a) Path deviation comparison. (b) Obstacle avoidance success rate. (c) Planning failure rate under adverse weather

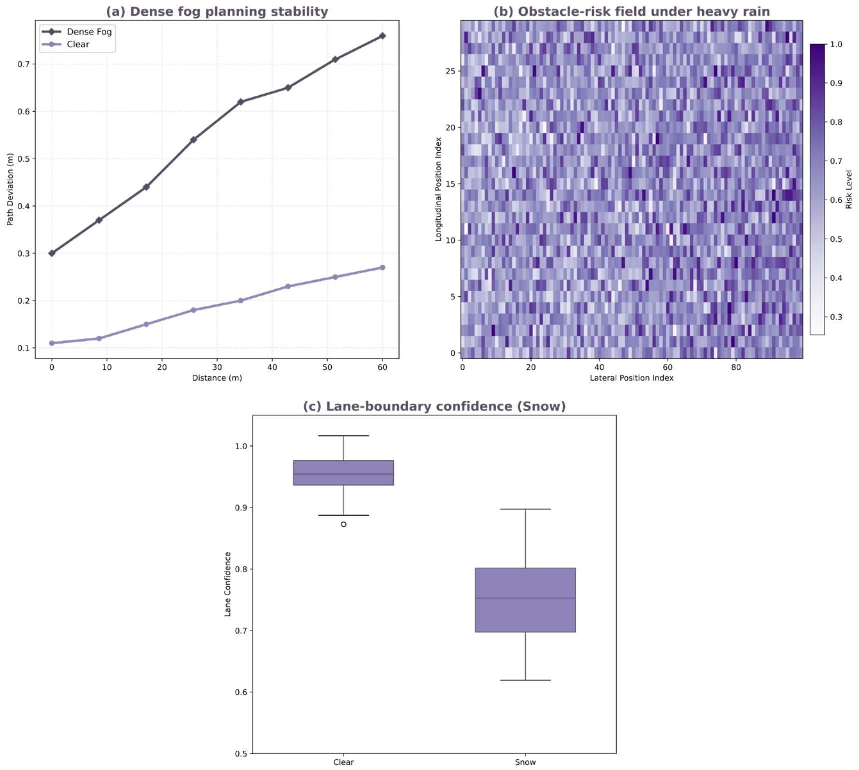

Figure 4. Robustness analysis under rain, fog, and snow disturbance. (a) Dense fog planning stability. (b) Heavy rain obstacle-risk response. (c) Snow-covered road boundary reliability

Instead of treating low-confidence lane regions as binary free space, the suggested planner views them as soft risk limitations. The design has decreased the near-miss rate from 11.2% to 5.3% in snow situations and from 9.8% to 4.1% in severe rain. Sensor fusion can improve robustness by lowering uncertainty in visually degraded environments, which is consistent with prior study on multi-modal adverse-weather perception [34]. The trajectory response and risk field are directly displayed in Figure 5. Figure 5(c) illustrates trajectory correction under uncertain perception, where the planned path shifts by 0.42m away from an ambiguous obstacle region while keeping the curvature below $0.18m^{-1}$; Figure 5(a) is the baseline risk field, which is primarily determined by detected obstacles and does not sufficiently consider weather uncertainty; Figure 5(b) is the proposed weather-aware risk field, which expands the area of uncertain obstacles and assigns a higher cost to low-visibility lanes.

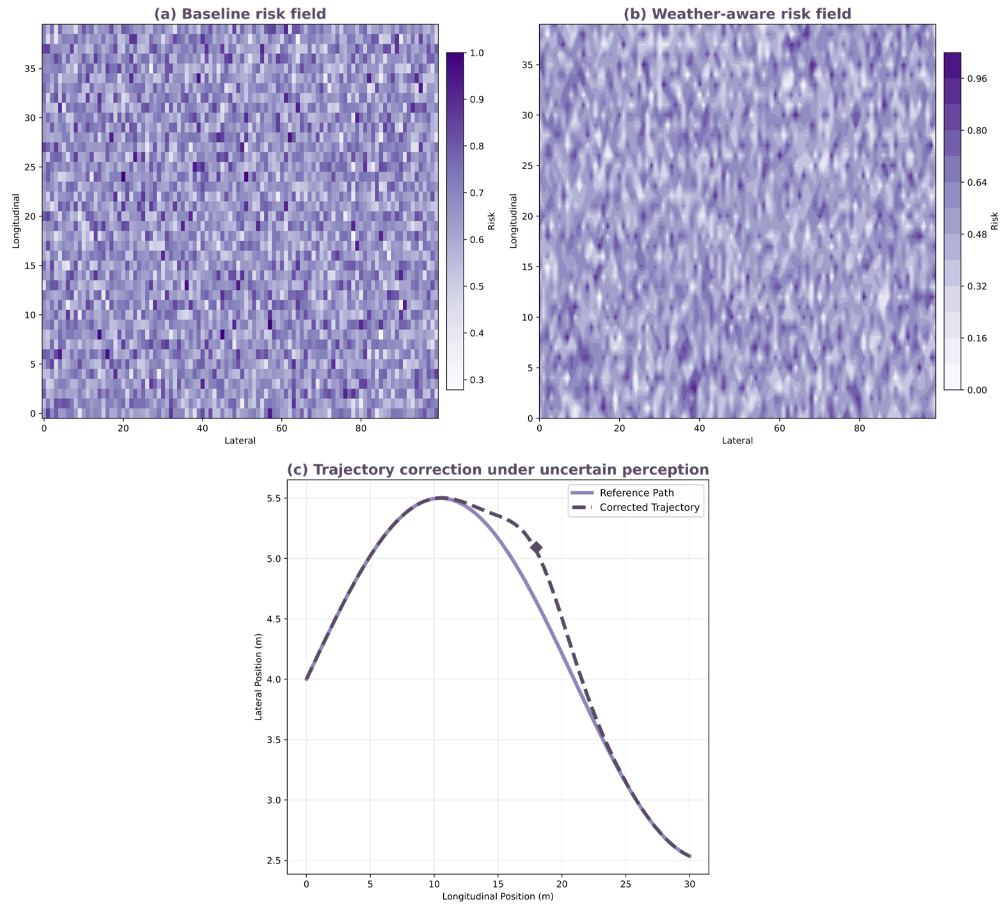

Figure 5. Risk field and trajectory response comparison. (a) Baseline risk field distribution. (b) Proposed weather-aware risk field. (c) Trajectory correction under uncertain perception

Risk response also demonstrates how the suggested approach increases safety without taking an overly cautious approach. The planner will only raise the cost when lane confidence, obstacle likelihood, and visibility decay all exhibit a significant level of uncertainty, rather than excluding all visually impaired locations in the event of severe rain. Uncertainty about the barriers should be transferred to the planning stage rather than disregarded in perception, as studies on rainy-condition object identification reveal that there are frequently false negatives and unstable bounding boxes in the presence of water streaks and road reflections [35]. Synthetic variety is only beneficial provided task-relevant labels are maintained and the structure necessary for downstream prediction is not harmed, according to research on picture data augmentation [36].

Ablation and Generalization Discussion

Test each component's impact separately. The generated adverse-weather images increase the domain coverage because the mean path deviation is 0.31m without GAN augmentation and rises to 0.39m after inclusion. The near-miss rate rises from 4.8% to 8.7% when the weather-aware risk representation is removed since the planner is no longer taking obstacle uncertainty and lane confidence into account. Robust Trajectory Optimization produces fewer stable pathways in low-adhesion situations and increases curvature variance by 23.5%. The generated samples are most useful when paired with task-specific constraints and distributional diversity, according to recent GAN studies [37]. The ablation results are displayed in Figure 6. Figure 6(a) displays the planning accuracy under various module combinations, Figure 6(b) displays the collision and near-miss rate following the removal of some crucial modules, and Figure 6(c) displays the change in planning latency brought about by trajectory optimization and risk-field computation.

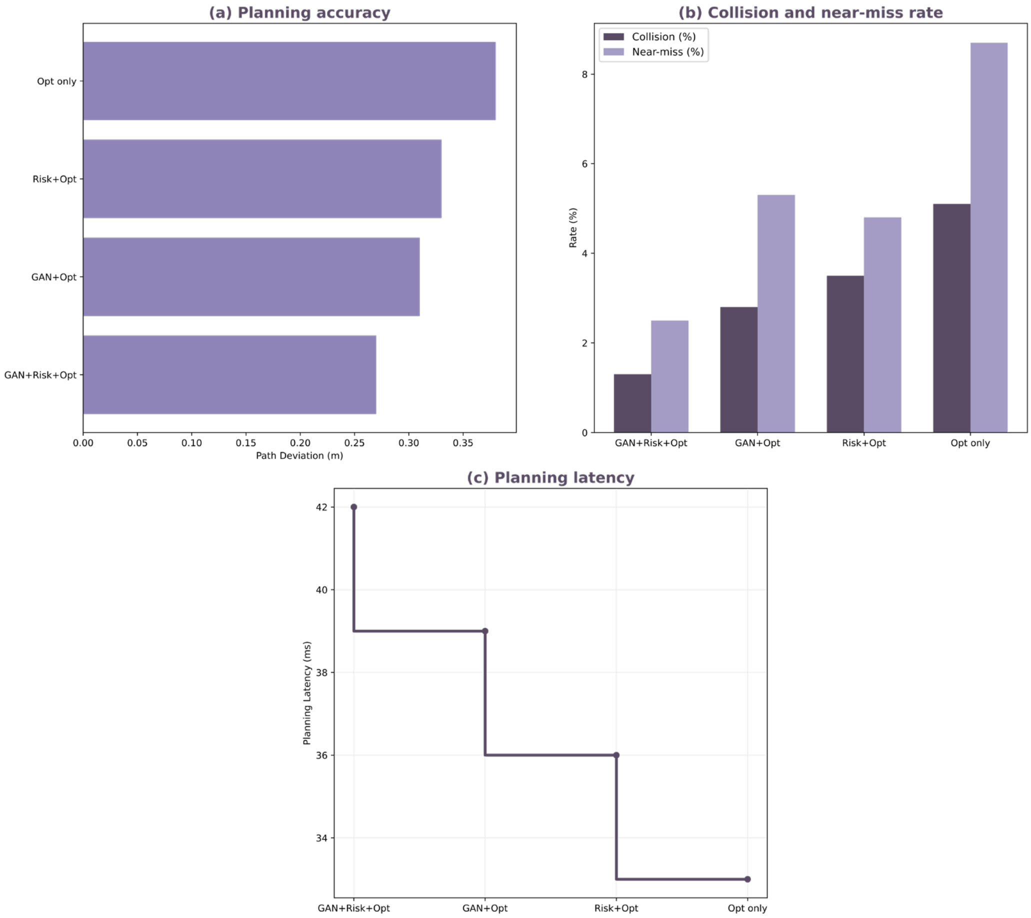

Figure 6. Ablation analysis of the proposed planning framework. (a) Planning accuracy under different module combinations. (b) Collision and near-miss rate comparison. (c) Planning latency comparison

The average planning latency is still 42 ms, which satisfies the real-time requirement of a 50 ms planning cycle, even if the entire model adds an additional 6.8 ms for the risk calculation. As a result, there will be less chance of collisions or near-misses even if there would be more computing. Generative models can enhance the robustness of downstream tasks while preserving structural consistency in synthesis, according to studies on image and video synthesis [38]. Examine cross-scene generalization using data from nighttime unfavorable weather, new urban roadways, and highways. This generalization performance is shown in Figure 7. Figure 7(a) assesses urban road scenes with parked cars and dense intersections; Figure 7(b) evaluates highway scenarios at a higher speed and with a longer perception distance; and Figure 7(c) compares the planning reliability and classification of nighttime adverse-weather conditions in unseen scenes.

The novel approach has a mean lateral deviation of 0.29m for highway scenarios, a success rate of 93.2% on unseen urban roadways, and a lower failure rate of 6.7% under severe weather at night compared to 13.5% for the non-GAN planner. Research on learning-based driving has demonstrated that scene diversity and policy reaction speed have an impact on closed-loop decision-making dependability [39]. According to an assessment of deep reinforcement learning applications in autonomous driving, diverse contexts must be introduced, safety costs must be clearly defined, and judgments must be continuously fed back in order for generalization to take place [40].

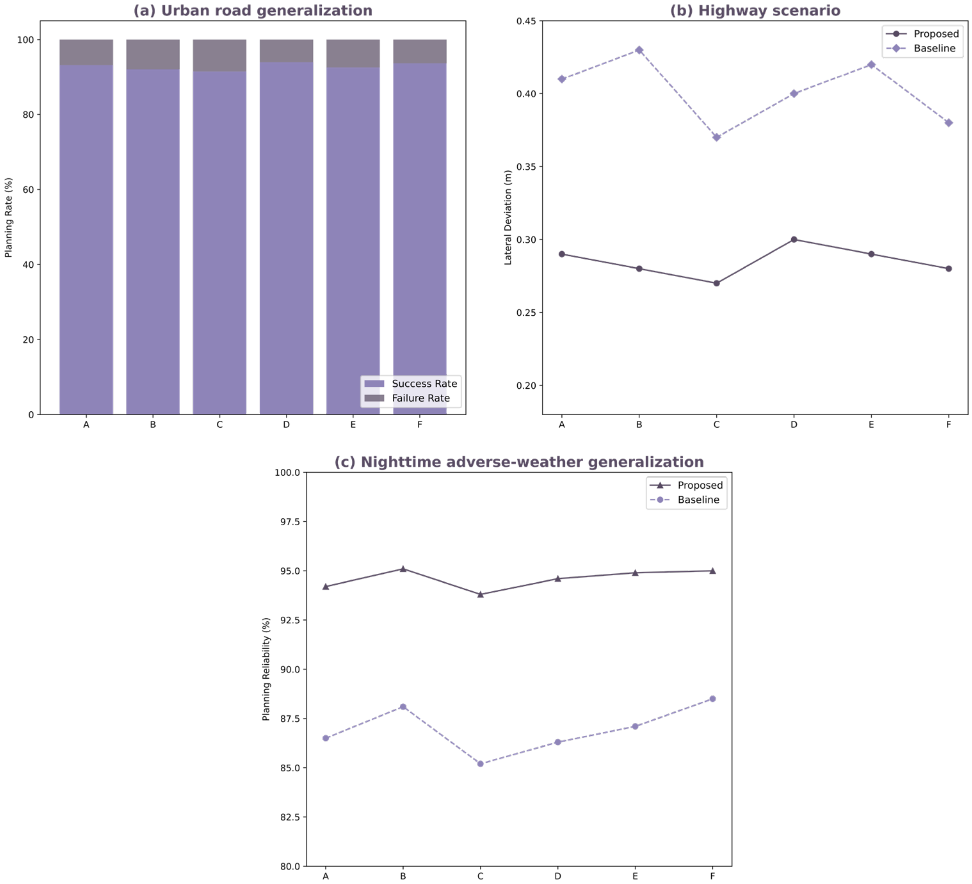

Figure 7. Cross-scene generalization under unseen weather conditions. (a) Urban road generalization. (b) Highway scenario generalization. (c) Nighttime adverse-weather generalization

Conclusion

This paper proposed a robust path planning framework for autonomous driving in bad weather that is augmented by GAN. The road structure and barrier arrangement are preserved while the rain, fog, snow, and low-light driving scenario sections are expanded via conditional adversarial generation. Create a weather-aware risk representation based on road-surface risk, obstacle likelihood, visibility attenuation, and lane confidence.

The experiment demonstrates that risk representation aids the planner in avoiding dangerous regions brought on by perception degradation, while adversarial weather augmentation strengthens the planner's resistance to distribution shift. In comparison to the baseline planner, the suggested approach has cut the average path variation, enhanced the obstacle avoidance success rate, and decreased the planning failure rate in conditions of dense fog, heavy rain, snow, and night.

The framework for weather-aware planning will be expanded in the future with additional LiDAR, radar, and vehicle-to-infrastructure data. To increase the practical dependability of autonomous driving systems in inclement weather, expand real-world closed-loop vehicle testing, add more diverse mixed-weather scenarios, and create end-to-end planning structures.

Author Contributions

Sabina Walczak contributes to conceptualization, methodology, software, validation, analysis, investigation, data collection, draft preparation, manuscript editing, visualization, supervision, project administration, and funding acquisition. Lidia Wójcikowa contributes to validation, analysis, investigation, data collection, draft preparation.

Patrycja Ostrowska contributes to validation, analysis. All authors have read and agreed with the manuscript before its submission and publication.

Funding

This research received no specific financial support from any funding agency.

Institutional Review Board Statement

Not applicable.

References

[1] Zang, S., Ding, M., Smith, D., Tyler, P., Rakotoarivelo, T., & Kaafar, M. A. (2019). The impact of adverse weather conditions on autonomous vehicles: How rain, snow, fog, and hail affect the performance of a self-driving car. IEEE Vehicular Technology Magazine, 14(2), 103-111. https://doi.org/10.1109/MVT.2019.2892497

[2] Yurtsever, E., Lambert, J., Carballo, A., & Takeda, K. (2020). A survey of autonomous driving: Common practices and emerging technologies. IEEE Access, 8, 58443-58469. https://doi.org/10.1109/ACCESS.2020.2983149

[3] Badue, C., Guidolini, R., Carneiro, R. V., Azevedo, P., Cardoso, V. B., Forechi, A., et al. (2021). Self-driving cars: A survey. Expert Systems with Applications, 165, 113816. https://doi.org/10.1016/j.eswa.2020.113816

[4] Grigorescu, S., Trasnea, B., Cocias, T., & Macesanu, G. (2020). A survey of deep learning techniques for autonomous driving. Journal of Field Robotics, 37(3), 362-386. https://doi.org/10.1002/rob.21918

[5] Claussmann, L., Revilloud, M., Gruyer, D., & Glaser, S. (2020). A review of motion planning for highway autonomous driving. IEEE Transactions on Intelligent Transportation Systems, 21(5), 1826-1848. https://doi.org/10.1109/TITS.2019.2913998

[6] El Mahdawy, M., & El Mougy, A. (2021). Path planning for autonomous vehicles with dynamic lane mapping and obstacle avoidance. Proceedings of the 13th International Conference on Agents and Artificial Intelligence, 431-438. https://doi.org/10.5220/0010342704310438

[7] Chu, K., Zhao, M., Bakshi, S., & Yan, X. (2021). Risk-aware path planning with uncertain human interactions. 2021 American Control Conference, 4225-4230. https://doi.org/10.23919/ACC50511.2021.9483314

[8] Chandra, R., Wang, T., Schwager, M., & Manocha, D. (2022). Game-theoretic planning for autonomous driving among risk-aware human drivers. 2022 International Conference on Robotics and Automation, 2876-2883. https://doi.org/10.1109/ICRA46639.2022.9811865

[9] Musat, V., Fursa, I., Newman, P., Cuzzolin, F., & Bradley, A. (2021). Multi-weather city: Adverse weather stacking for autonomous driving. 2021 IEEE/CVF International Conference on Computer Vision Workshops, 2906-2915. https://doi.org/10.1109/ICCVW54120.2021.00325

[10] Dhananjaya, N., Kumar, S., & Yogamani, S. (2021). Weather and light level classification for autonomous driving: Dataset, baseline and active learning. 2021 IEEE International Intelligent Transportation Systems Conference, 2816-2821. https://doi.org/10.1109/ITSC48978.2021.9564689

[11] Lee, S., Shiotsuka, D., Nishimori, T., & Nakao, M. (2022). GAN-based LiDAR translation between sunny and adverse weather for autonomous driving and driving simulation. Sensors, 22(14), 5287. https://doi.org/10.3390/s22145287

[12] Lee, H., Ko, H., Kim, J., & Jeon, M. (2022). Perception-friendly video enhancement for autonomous driving under adverse weather conditions. 2022 International Conference on Robotics and Automation, 7760-7767. https://doi.org/10.1109/ICRA46639.2022.9811870

[13] Arnelid, H., Zec, E. L., & Mohammadiha, N. (2019). Recurrent conditional generative adversarial networks for autonomous driving sensor modelling. 2019 IEEE Intelligent Transportation Systems Conference, 1613-1618. https://doi.org/10.1109/ITSC.2019.8916999

[14] Vinod, K., Prabhakar, R. R., Babu, R. V., & Chakraborty, A. (2021). Multi-domain conditional image translation: Translating driving datasets from clear-weather to adverse conditions. 2021 IEEE/CVF International Conference on Computer Vision Workshops, 1571-1582. https://doi.org/10.1109/ICCVW54120.2021.00182

[15] Kwak, J., Jin, Y., Li, Y., & Yoon, K. J. (2021). Adverse weather image translation with asymmetric and uncertainty-aware GAN. Proceedings of the British Machine Vision Conference 2021, 396. https://doi.org/10.5244/C.35.396

[16] Bihlo, A. (2021). A generative adversarial network approach to ensemble weather prediction. Neural Networks, 139, 1-16. https://doi.org/10.1016/j.neunet.2021.02.003

[17] Zhang, Y., Wang, J., & Meng, M. Q. H. (2022). Generative adversarial network-based heuristics for sampling-based path planning. IEEE/CAA Journal of Automatica Sinica, 9(1), 64-74. https://doi.org/10.1109/JAS.2021.1004275

[18] Liniger, A., & Van Gool, L. (2020). Safe motion planning for autonomous driving using an adversarial road model. Robotics: Science and Systems XVI. https://doi.org/10.15607/RSS.2020.XVI.044

[19] Li, Y., Zhou, Z., Pu, Z., & Yu, H. (2021). Multi-modal neural feature fusion for automatic driving through perception-aware path planning. IEEE Access, 9, 142782-142794. https://doi.org/10.1109/ACCESS.2021.3120720

[20] Qiao, Y., Pollmeyer, B., Wang, W., & Fleps-Dezasse, M. (2020). Model predictive trajectory planning of autonomous vehicles considering dynamic driving constraints. 2020 CAA International Conference on Vehicular Control and Intelligence, 136-141. https://doi.org/10.1109/CVCI51460.2020.9338480

[21] Shi, Y., Sun, X., Qin, Y., & Hu, C. (2020). Planning the trajectory of an autonomous wheel loader and tracking its trajectory via adaptive model predictive control. Robotics and Autonomous Systems, 131, 103570. https://doi.org/10.1016/j.robot.2020.103570

[22] Xue, Z., Zhong, Z., & Li, Y. (2022). A model predictive trajectory planning framework for autonomous ground vehicles on structured and unstructured roads. 2022 IEEE International Conference on Intelligent Transportation Systems, 1458-1463. https://doi.org/10.1109/ITSC55140.2022.9921808

[23] Vosahlik, M., Turnovec, S., Pekar, L., & Hanis, T. (2022). Vehicle trajectory planning: Minimum violation planning and model predictive control comparison. 2022 IEEE Intelligent Vehicles Symposium, 145-150. https://doi.org/10.1109/IV51971.2022.9827430

[24] Zuo, L., Li, Y., & Wang, L. (2020). Behavior assessment and trajectory planning for autonomous vehicles on structural urban roads. 2020 Chinese Control Conference, 5683-5688. https://doi.org/10.23919/CCC50068.2020.9189597

[25] Viana, I. B., Kanchwala, H., & Aouf, N. (2019). Cooperative trajectory planning for autonomous driving using nonlinear model predictive control. 2019 IEEE International Conference on Connected Vehicles and Expo, 1-6. https://doi.org/10.1109/ICCVE45908.2019.8965227

[26] Dong, X., Yu, H., & Xi, J. (2022). Real-time model predictive control for simultaneous drift and trajectory tracking of autonomous vehicles. 2022 CAA International Conference on Vehicular Control and Intelligence, 1-6. https://doi.org/10.1109/CVCI56766.2022.9964790

[27] Chen, H., Mu, Y., & Zhao, Y. (2020). Trajectory planning for autonomous vehicles at autonomous intersection. CICTP 2020, 332-342. https://doi.org/10.1061/9780784482933.029

[28] Ha, J., Kim, H., & Park, J. (2022). Object recognition for autonomous driving in adverse weather condition using polarized camera. 2022 International Conference on Control, Mechatronics and Automation, 42-46. https://doi.org/10.1109/ICCMA56665.2022.10011462

[29] Gao, Z., Roy, S., Xing, Y., & Jin, X. (2021). Perception through 2D-MIMO FMCW automotive radar under adverse weather. 2021 IEEE International Conference on Autonomous Systems, 1-5. https://doi.org/10.1109/ICAS49788.2021.9551127

[30] Nagiub, M., & Beuth, F. (2022). Towards depth perception from noisy camera-based sensors for autonomous driving. Proceedings of the 8th International Conference on Vehicle Technology and Intelligent Transport Systems, 198-207. https://doi.org/10.5220/0010989800003191

[31] Pareigis, M., & Maass, W. (2022). Robust neural network for sim-to-real gap in end-to-end autonomous driving. Proceedings of the 19th International Conference on Informatics in Control, Automation and Robotics. https://doi.org/10.5220/0011140800003271

[32] Ji, Y., Yang, X., Wang, Y., & Zhu, J. (2021). A driving risk prediction approach based on generative adversarial networks and VANET for autonomous trams. 2021 International Conference on Networking and Network Applications, 520-526. https://doi.org/10.1109/NaNA53684.2021.00096

[33] Sakaridis, C., Dai, D., & Van Gool, L. (2021). ACDC: The adverse conditions dataset with correspondences for semantic driving scene understanding. 2021 IEEE/CVF International Conference on Computer Vision, 10745-10755. https://doi.org/10.1109/ICCV48922.2021.01059

[34] Bijelic, M., Gruber, T., Mannan, F., Kraus, F., Ritter, W., Dietmayer, K., & Heide, F. (2020). Seeing through fog without seeing fog: Deep multimodal sensor fusion in unseen adverse weather. 2020 IEEE/CVF Conference on Computer Vision and Pattern Recognition, 11679-11689. https://doi.org/10.1109/CVPR42600.2020.01170

[35] Hnewa, M., & Radha, H. (2021). Object detection under rainy conditions for autonomous vehicles: A review of state-of-the-art and emerging techniques. IEEE Signal Processing Magazine, 38(1), 53-67. https://doi.org/10.1109/MSP.2020.2984801

[36] Shorten, C., & Khoshgoftaar, T. M. (2019). A survey on image data augmentation for deep learning. Journal of Big Data, 6, 60. https://doi.org/10.1186/s40537-019-0197-0

[37] Pan, Z., Yu, W., Yi, X., Khan, A., Yuan, F., & Zheng, Y. (2019). Recent progress on generative adversarial networks (GANs): A survey. IEEE Access, 7, 36322-36333. https://doi.org/10.1109/ACCESS.2019.2905015

[38] Liu, M. Y., Huang, X., Yu, J., Wang, T. C., & Mallya, A. (2021). Generative adversarial networks for image and video synthesis: Algorithms and applications. Proceedings of the IEEE, 109(5), 839-862. https://doi.org/10.1109/JPROC.2021.3049196

[39] Kendall, A., Hawke, J., Janz, D., Mazur, P., Reda, D., Allen, J. M., et al. (2019). Learning to drive in a day. 2019 International Conference on Robotics and Automation, 8248-8254. https://doi.org/10.1109/ICRA.2019.8793742

[40] Kiran, B. R., Sobh, I., Talpaert, V., Mannion, P., Al Sallab, A. A., Yogamani, S., & Perez, P. (2022). Deep reinforcement learning for autonomous driving: A survey. IEEE Transactions on Intelligent Transportation Systems, 23(6), 4909-4926. https://doi.org/10.1109/TITS.2021.3054625